Author Version of : Geo-Marine Letters, vol.38(4); 2018; 341-350

Variability of terrigenous input to the Bay of Bengal for the last ~80 kyr: Implications on the Indian monsoon variability

Champoungam Panmei[1,2], Pothuri Divakar Naidu[1], Sushant Suresh Naik[1]

[1] CSIR - National Institute of Oceanography (CSIR-NIO), Dona Paula, Goa 403004, India.
[2] Academy of Scientific and Innovative Research (AcSIR), CSIR-NIO, Goa 403004, India.
Corresponding author: cpanmei@nio.org (C. Panmei)
ORCID: C. Panmei - 0000-0003-4907-2155

Abstract

Oceanographic processes in the Bay of Bengal (BoB) are strongly impacted by south-westerly and north-easterly winds of the Indian monsoon system during the summer and winter respectively. Variations in calcium carbonate ($CaCO_3$) content and magnetic susceptibility (MS), along with Ba, Ti, and Al, were reconstructed for the past ~80 kyr using a sediment core (MD 161/28) from the northern BoB in order to understand the changes in calcium carbonate deposition and MS signals associated with the Indian monsoon system. Our records infer monsoon-induced dilution through river discharges from different sediment provenance to be the main controlling factor of the $CaCO_3$ variations at the core location. Generally lower $CaCO_3$ content during stronger-southwest monsoon (SWM) interglacial periods (Marine Isotope Stage (MIS) 5a & 1, except 3) and higher $CaCO_3$ content during weaker-SWM glacial periods (MIS 4 & 2) were documented. High MS correspond to MIS 4 & 2 of weakened SWM and strengthened northeast monsoon (NEM) periods caused due to enhanced sediment supply from the Peninsular Indian regions, whereas lower MS values correspond to MIS 5, 3 & 1 of strengthened SWM and weakened NEM derived through Ganges-Brahmaputra from the Himalaya Region. Thus, our records infer coupling of major rivers' discharges to the BoB with the SWM and NEM strengths, which has implications on the linkage with other climatic variations such as East Asian monsoon and Northern Hemisphere climate.

Formatted: Font: 12 pt, Not Bold, Italic, Complex Script Font: 12 pt
Formatted: Font: 12 pt, Italic, Complex Script Font: 12 pt
Formatted: Font: (Default) Times New Roman, 12 pt, Italic, Complex Script Font: Times New Roman, 12 pt
Formatted: Left, Line spacing: Multiple 1.15 li
Formatted: Font: 12 pt, Italic, Complex Script Font: 12 pt
Formatted: Left: 0.75", Right: 0.75", Header distance from edge: 0.5", Footer distance from edge: 0.5"
Formatted: Font: 13 pt, Complex Script Font: 13 pt
Formatted: Line spacing: Multiple 1.15 li
Formatted: Level 1, Space After: 0 pt, Line spacing: single
Formatted: Font: 11 pt, Not Bold, Complex Script Font: 11 pt
Formatted: Space After: 0 pt
Formatted: Space After: 0 pt, Line spacing: single
Formatted: Font: 11 pt, Not Bold, No underline, Font color: Custom Color(RGB(0,0,10)), Complex Script Font: 11 pt, (Complex) Hindi, English (India)
Formatted: Font: 11 pt, Not Bold, Complex Script Font: 11 pt
Formatted: Font: 11 pt, Not Bold, No underline, Font color: Custom Color(RGB(0,0,10)), Complex Script Font: 11 pt, (Complex) Hindi, English (India)
Formatted: Font: 11 pt, Not Bold, Complex Script Font: 11 pt
Formatted: Font: 12 pt, Complex Script Font: 12 pt
Formatted: Space After: 6 pt, Line spacing: single
Formatted: Font: 12 pt, Complex Script Font: 12 pt
Formatted: Level 1, Space After: 6 pt, Line spacing: single
Formatted: Space After: 6 pt, Line spacing: single
Formatted: No underline, Font color: Custom Color(RGB(0,0,10)), (Complex) Hindi, English (India)

Introduction

The Indian monsoon is one of the most important climate systems of the world, responsible for transportation and redistribution of a huge amount of heat and moisture in the Indian Ocean (Webster et al. 1998). Temperature and pressure differences over the Asian continent and the Indian Ocean drive the monsoonal circulation; alternating wind patterns develop with southwesterly winds during summer and northeasterly winds during winter as a response to the migration of the intertropical convergence zone (ITCZ) driven by insolation of the Indian subcontinent and Tibetan Plateau (Chao 2000; Chao and Chen 2001; Gadgil 2003). The southwest monsoon (SWM), which occurs during the northward migration of the ITCZ, during northern Hemisphere summer induces wind-stress curl-driven upwelling offshore and upwelling of cold, nutrient-rich waters in western and southeastern Arabian Sea (e.g., Webster et al. 1998), and brings in a huge amount of precipitation and river outflow from Ganges-Brahmaputra to the BoB during summer (Shetye 1993; Sengupta et al. 2006). In Boreal winter, the wind reverses in direction occurring during the southward migration of the ITCZ and the resultant northeasterly winds produce drier conditions over the Indian region; the northeast monsoon (NEM) winds, lower in intensity and less-moisture laden, induce convective mixing in the northeastern Arabian Sea and cooling of the northern BoB.

Surface ocean circulation in the Bay of Bengal is driven primarily by the Indian monsoon (e.g., Schott and McCreary 2001). Though located along the same latitudinal belt, the Arabian Sea and the BoB, the latter is influenced by a more intense rainfall, fresher surface waters and haline stratification (e.g., Madhupratap et al. 2003). BoB receives 1300 km^3 of freshwater (UNESCO reports 1971; Rao 1979) and suspended sediments of over 1350 million tons every year (Milliman and Meade 1983; Subramaniam 1985; Anon 1993) from various sources such as the Himalayas, Trans-Himalayan Plutonic Belt, Indo-Burman ranges and the Peninsular India through the major rivers Ganga, Brahmaputra, Irrawaddy, Salween, Godavari, Mahanadi and Krishna (Tripathy et al. 2011). These rivers contribute roughly equally to the total freshwater received by the BoB, north of 15°N and create a low sea surface salinity resulting in a near-surface haline stratification (Akhil et al., 2014) which plays an important role in maintaining the northern Indian Ocean climate (Shenoi et al., 2002). Furthermore, the river discharges to the BoB from these different source basins vary accordingly to the change in the intensity of the monsoon systems (SWM and NEM), implying that

Formatted: No underline, Font color: Custom Color(RGB(0,0,10)), (Complex) Arabic (Saudi Arabia), English (United Kingdom)

Formatted: Justified, Space After: 6 pt, Line spacing: 1.5 lines

Formatted: No underline, Font color: Custom Color(RGB(0,0,10)), (Complex) Hindi, English (India)

Formatted: Space After: 6 pt, Line spacing: 1.5 lines

Formatted: No underline, (Complex) Hindi, English (India)

Formatted: No underline, Font color: Custom Color(RGB(0,0,10)), (Complex) Hindi, English (India)

Formatted: No underline

Formatted: No underline, Font color: Custom Color(RGB(0,0,10))

Formatted: No underline

Formatted: No underline, Font color: Custom Color(RGB(0,0,10)), (Complex) Hindi, English (India)

Formatted: No underline, Font color: Custom Color(RGB(0,0,10))

Formatted: No underline, Font color: Custom Color(RGB(0,0,10)), (Complex) Hindi, English (India)

Formatted: No underline, (Complex) Hindi, English (India)

Formatted: No underline, Font color: Custom Color(RGB(0,0,10))

Formatted: No underline, (Complex) Hindi, English (India)

Formatted: Font: 12 pt, Complex Script Font: 12 pt

Formatted: Justified, Space After: 6 pt, Line spacing: 1.5 lines

Formatted: Space After: 6 pt, Line spacing: 1.5 lines

Formatted: No underline, (Complex) Hindi, English (India)

Formatted: No underline, Font color: Custom Color(RGB(0,0,10)), (Complex) Hindi, English (India)

Formatted: No underline, (Complex) Hindi, English (India)

Formatted: No underline, Font color: Custom Color(RGB(0,0,10)), (Complex) Hindi, English (India)

studying the variations in the sediment would give an insight into changes in the monsoon intensity. The present study is based on a sediment core from the northern BoB which is impacted by both Ganges-Brahmaputra and Mahanadi river systems. To the BoB, the Ganges-Brahmaputra alone contributes freshwater discharge of ~30742 m^3s^{-1} and ~1 x 10^9 tonnes of sediment per year, while Mahanadi's contribution is ~2113 m^3s^{-1} of freshwater discharge and ~60 x 10^6 tonnes of sediment per year (Milliman and Meade 1983; Ahmad et al. 2009; Tripathy et al. 2011).

Calcium carbonate ($CaCO_3$) content of deep-sea sediments has long been known to fluctuate in response to Quaternary climate changes such as glacial and interglacial conditions (Damuth 1975). The $CaCO_3$ content in marine sediment is controlled by the interplay of three parameters: productivity of carbonate-secreting organisms, dilution by the non-carbonate fraction and terrigenous matter and carbonate removal by dissolution on the seafloor. The individual contribution of these parameters is highly variable in different regions. Generally, in the regions of river mouths, the $CaCO_3$ content is mainly controlled by the terrigenous dilution in the Indian Ocean (e.g., Naidu 1991; Pattan et al. 2003). Also, low salinity conditions and sediment plumes occurring near the near river mouths due to monsoon-associated river discharges have been known to control the $CaCO_3$ content by hindering light availability thereby ultimately reducing primary productivity (Gomes et al. 2000; Prasanna Kumar et al., 2002; Madhupratap et al. 2003). Magnetic susceptibility (MS) in sediments, on the other hand, is related to their total magnetic mineral concentrations and, in general, is an expression of terrigenous input. Magnetic grain-size variations and post-depositional alteration of magnetic minerals, both authigenic and diagenetic, have also been known to control the MS values as well (Sager and Hall 1990; Weber et al. 2003). However, in general, MS variations down core in sediments correlate with changes in climatic patterns such as weathering, monsoon-associated precipitation-induced run-off and terrigenous input, and aridity/humidity. Previous studies have correlated magnetic susceptibility to climatic records in deep-sea sediments; for instance, Kent (1982) reported a high significance of the high inverse correlation between magnetic susceptibility and $CaCO_3$ from a southern Indian Ocean deep-sea core. Similarly, MS was used a proxy to reconstruct the terrigenous input in the Arabian Sea (e.g., deMenocal et al. 1991; Kumar et al. 2005; Rao et al. 2008, 2010) and correlated it directly to terrigenous percent through continental inputs along the west coasts of India, rather than dilution by variations in biogenic input or other post-depositional processes. Also, magnetic susceptibility has been as a useful proxy of detrital processes influenced by the Indian monsoon (e.g. Colin et al., 1998; Phillips et al., 2014). Interestingly, unlike in the Arabian Sea, MS showed a certain degree of co-variability with $CaCO_3$ in the BoB, which was

attributed to relative contribution from Ganges-Brahmaputra and peninsular rivers associated with the strength of monsoon (e.g., Phillips et al. 2014).

A relatively higher amount of work has been done on calcium carbonate and magnetic susceptibility of sediments from the Arabian Sea in comparison to the BoB. The Indian monsoon dynamics being very complex and variable in time and space, the findings from the Arabian Sea cannot explain the terrigenous input variations through time in the BoB. Therefore here, an attempt has been made to understand the terrigenous material variability in the BoB over the last ~80 kyr.

Materials and Methods

Core and chronology

The piston Core MD 161/28 was collected onboard the Research Vessel Marion Dufresne during 2007 at a water depth of 1359 m from the northern BoB (19°50'N, 87°59'E) (Fig. 1) with a total length of 36.25 m retrieved, located off the river mouth of Mahanadi in the west and Ganges-Brahmaputra to the north. For the present study, the core was sampled at 5 cm intervals for magnetic susceptibility and 25 cm intervals for $CaCO_3$ content up to 10.44 m and the rest stored in CSIR-NIO's repository. The chronology of this core was established based on 12 ^{14}C AMS dates performed on monospecific planktonic foraminifera species *Globigerinoides ruber* at the AMS facility of the University of Arizona, USA. Chronology from 600 to 1044 cm depth was derived from the ascribed ages of Marine Isotope Stage boundaries of 3 and 4, 4 and 5, and 5.1 of $\delta^{18}O$ data from the same Core MD161/28 (Naidu et al., 2018 in preparation). The measured ^{14}C dates were calibrated to calendar ages using the calibration program Calib 7.1 and Marine13 calibration curve (Stuiver and Reimer 1993; Reimer et al. 2013), with a global reservoir correction of 400 years based on observations for the Indian Ocean (Southon et al. 2002) (also see Table S1 in Supplementary Material). Age model derived by the calibrated ^{14}C ages and MIS derived ages are shown against the depth in Fig. 2 along with 2σ uncertainties. Ages between the tie points were obtained by linear interpolation. Sedimentary rates varied in the range of ~7.1 – 62.5 cm/kyr. Sediment colour variations in the core were noted during sub-sampling using a rock colour chart, which are also shown alongside the core depth in Fig. 2.

Calcium carbonate content

$CaCO_3$ content was determined using the technique of weight loss by acidification following Carver (1971). It was done by calculating the mass difference resulting from treatment of the sediment samples with a dilute acid i.e. 2N HCl. The calculation is done using the equation: $CaCO_3$ (wt%) =

Formatted: No underline, Font color: Custom Color(RGB(0,0,10)), (Complex) Hindi, English (India)
Formatted: Space Before: 0 pt, After: 6 pt, Line spacing: 1.5 lines
Formatted: No underline, (Complex) Hindi, English (India)
Formatted: Font: 12 pt, Complex Script Font: 12 pt
Formatted: Indent: First line: 0.5", Space After: 6 pt, Line spacing: 1.5 lines
Formatted: Space After: 6 pt, Line spacing: 1.5 lines
Formatted: No underline, (Complex) Hindi, English (India)
Formatted: No underline, (Complex) Hindi, English (India)
Formatted: No underline, (Complex) Hindi
Formatted: No underline, (Complex) Hindi, English (India)
Formatted: No underline, (Complex) Hindi
Formatted: No underline, (Complex) Hindi, English (India)
Formatted: No underline, Font color: Custom Color(RGB(0,0,10)), (Complex) Hindi, English (India)
Formatted: No underline, (Complex) Hindi, English (India)
Formatted: No underline, Font color: Custom Color(RGB(0,0,10)), (Complex) Hindi, English (India)
Formatted: No underline, (Complex) Hindi, English (India)
Formatted: Font: 12 pt, No underline, Complex Script Font: 12 pt, (Complex) Hindi, English (India)
Formatted: No underline, (Complex) Hindi, English (India)
Formatted: No underline, Font color: Custom Color(RGB(0,0,10)), (Complex) Hindi, English (India)
Formatted: No underline, Font color: Custom Color(RGB(0,0,10)), (Complex) Hindi, English (India)
Formatted: No underline, Font color: Custom Color(RGB(0,0,10)), (Complex) Hindi, English (India)
Formatted: No underline, (Complex) Hindi, English (India)
Formatted: No underline, Font color: Custom Color(RGB(0,0,10)), (Complex) Hindi, English (India)

(Weight of sample after acidification/Weight of sample before acidification)*100. The precision obtained on $CaCO_3$ using on in-house reference material is □1 % (1σ; n=10).

Magnetic susceptibility

Magnetic susceptibility measurements on the samples were made using a Bartington MS-2 magnetic susceptibility meter at the Paleomagnetism Lab, CSIR – National Institute of Oceanography (NIO), Goa, India. Representative samples were air-dried and packed into 1 cm^3 cylindrical pots. Low-frequency (0.465 kHz) and high-frequency (4.65 kHz) magnetic susceptibilities were measured 3 times on each sample and the average of 3 measurements were presented as volume specific values in 10^{-5} SI units.

Ba, Ti and Al

0.05g of dried sediment was powdered by using agate mortar and pestle, and later subjected to open-vessel acid digestion technique with 7:3:1 solution of $HF\text{-}HNO_3\text{-}HClO_4$ (adopted from Totland et al. 1992). The sample preparation was carried out at Geochemistry Lab, CSIR-NIO, Goa, India. The prepared samples were analyzed for Barium, Titanium, and Aluminium by using Agilent Technologies 700 Series inductively coupled plasma-optical emission spectrometer (ICP-OES) at Chemical Oceanography Division, CSIR-NIO, Goa, India.

Results

Calcium carbonate content

The $CaCO_3$ values range from 11.7 to 24.9 wt% over the last ~80 kyr (Fig. 3). $CaCO_3$ values were very low in MIS 5a with an average of ~13 wt% which is similar to MIS 1. An increasing trend is observed in MIS 4, the values varying from ~11.8-18.9 wt% with an average of ~16.3 wt%. MIS 3 has a much higher average value of 20.8 wt%. MIS 2 recorded the highest range of values from 18.8 to 23.9wt% with an average of 21.4 wt%. A rapid decrease in the values is observed at the onset of MIS 1 to reach a minimum of 11.7 wt% at ~6.8 kyr with an average of 13.7 wt%, the lowest of all the periods.

Magnetic Susceptibility (MS)

Formatted: No underline, (Complex) Hindi, English (India)

Formatted: Font: Times New Roman, No underline, (Complex) Hindi, English (India)

Formatted: No underline, (Complex) Hindi, English (India)

Formatted: No underline, (Complex) Hindi, English (India)

Formatted: None, Space After: 6 pt, Line spacing: 1.5 lines

Formatted: No underline, (Complex) Hindi, English (India)

Formatted: Space After: 6 pt, Line spacing: 1.5 lines

Formatted: No underline, (Complex) Hindi, English (India)

Formatted: Font: 12 pt, Not Bold, Complex Script Font: 12 pt

Formatted: Normal, None, Space After: 6 pt

Formatted: Space After: 6 pt

Formatted: No underline, Font color: Custom Color(RGB(0,0,10)), (Complex) Arabic (Saudi Arabia), English (United Kingdom)

Formatted: Space After: 6 pt, Line spacing: 1.5 lines

Formatted: No underline, Font color: Custom Color(RGB(0,0,10)), (Complex) Arabic (Saudi Arabia), English (United Kingdom)

Formatted: No underline, (Complex) Arabic (Saudi Arabia), English (United Kingdom)

Formatted: No underline, Font color: Custom Color(RGB(0,0,10)), (Complex) Arabic (Saudi Arabia), English (United Kingdom)

Formatted: No underline, Font color: Custom Color(RGB(0,0,10)), (Complex) Arabic (Saudi Arabia), English (United Kingdom)

The MS values, both low and high frequency, follow closely each other in terms of values and trend that they are almost identical. Their values range from 5.42 to 33.38(10^{-5} SI) over the past ~80 kyr at this location (Fig. 3). Lowest MS values are recorded in MIS 5a except for a peak of 11.3(10^{-5} SI) at ~78 kyr but increased towards the end varying from 5.6(10^{-5} SI) at ~77.7 kyr to 14.4(10^{-5} SI) at ~72.5 kyr. MIS 4 values remain high with an average value of ~14.7(10^{-5} SI). In MIS 3, the variability of MS values show no specific pattern or trend, but with central values in a low range varying from ~9-13(10^{-5} SI) except for a peak of 20.9(10^{-5} SI) at ~45.6 kyr and abrupt increase at the end to a maximum of 33.4(10^{-5} SI) at ~26.8 kyr. MIS 2 witnessed an overall decreasing trend of MS values, although it also recorded a prominent peak of 28.17(10^{-5} SI) observed at ~19.7 kyr. The transition from MIS 2 to 1 continued with a decreasing trend of the MS values till mid-Holocene (~6-7 kyr), after which a gradual, increasing trend is noticed.

Ba, Ti and Al

Ba shows generally higher values during MIS 5a, 3 and 1, and lower during MIS 4 & 2. The values dropped from 485 ppm at ~76.7 kyr to an average of 403.8 ppm during MIS 4 (Fig. 3). During MIS 3, Ba values varied with an average of ~406 ppm. MIS 2 documented an increasing pattern of Ba values while MIS 1 recorded the highest with an average of ~519 ppm. On the other hand, Ti values increased from MIS 5a to 4 (~0.39 – 0.43 wt%) but remained low in MIS 3 with an average of 0.40 wt% except for an increasing trend towards its end (Fig. 3). Ti values decreased from the end of MIS 3 (~0.44 wt% at ~26 kyr) through MIS 2 to early MIS 1. Then, the values sharply increased till the present day; from ~0.37 wt% at ~9 kyr to ~0.44 wt% at ~1.1 kyr. Al shows highly fluctuating values for the past ~80 kyr. Al values decreased from MIS 5 to 4, and further to 3, but showed increasing trend from 6.7 wt% at ~52.7 kyr to 8.8 wt% at ~28 kyr (Fig. 3). Al in MIS 2 gradually increased from ~8.5 to ~9.5 wt% at ~22 and ~12 kyr respectively, with an average value of ~9 wt%. During MIS 1, Al shows highest values with an average of ~9.5 wt%.

Discussion

Fluctuations of $CaCO_3$ and MS

MD 161/28 core is retrieved from a water depth (1359 m) and lies to the northwest of the core NGHP-01-19B (Phillips et al., 2014). Both these cores lie at depths shallower to the Bengal Fan depth and hence the sedimentation in both cases should be mainly influenced by peninsular Indian margin processes (see Phillips et al., 2014). The MD 161/28 is also shallower than the regional modern lysocline depth (~2600 m) in the BoB (Chen et al. 1995) and therefore the role of $CaCO_3$

Formatted: No underline, Font color: Custom Color(RGB(0,0,10)), (Complex) Arabic (Saudi Arabia), English (United Kingdom)

Formatted: No underline, (Complex) Arabic (Saudi Arabia), English (United Kingdom)

Formatted: No underline, Font color: Custom Color(RGB(0,0,10)), (Complex) Arabic (Saudi Arabia), English (United Kingdom)

Formatted: No underline, (Complex) Arabic (Saudi Arabia), English (United Kingdom)

Formatted: No underline, Font color: Custom Color(RGB(0,0,10)), (Complex) Arabic (Saudi Arabia), English (United Kingdom)

Formatted: No underline, (Complex) Arabic (Saudi Arabia), English (United Kingdom)

Formatted: No underline, Font color: Custom Color(RGB(0,0,10)), (Complex) Arabic (Saudi Arabia), English (United Kingdom)

Formatted: No underline, (Complex) Arabic (Saudi Arabia), English (United Kingdom)

Formatted: No underline, Font color: Custom Color(RGB(0,0,10)), (Complex) Arabic (Saudi Arabia), English (United Kingdom)

Formatted: No underline, (Complex) Arabic (Saudi Arabia), English (United Kingdom)

Formatted: No underline, Font color: Custom Color(RGB(0,0,10)), (Complex) Arabic (Saudi Arabia), English (United Kingdom)

Formatted: No underline, (Complex) Arabic (Saudi Arabia), English (United Kingdom)

Formatted: No underline, Font color: Custom Color(RGB(0,0,10)), (Complex) Arabic (Saudi Arabia), English (United Kingdom)

Formatted: No underline, (Complex) Arabic (Saudi Arabia), English (United Kingdom)

Formatted ... [1]

Formatted ... [2]

Formatted ... [3]

Formatted ... [4]

Formatted ... [5]

Formatted ... [6]

Formatted ... [7]

Formatted ... [8]

Formatted ... [9]

Formatted ... [10]

Formatted ... [11]

Formatted: None, Space After: 6 pt, Line spacing: 1.5 lines

Formatted ... [12]

Formatted: Space After: 6 pt, Line spacing: 1.5 lines

Formatted ... [13]

Formatted ... [14]

Formatted ... [15]

Formatted ... [16]

dissolution maybe negligible. Furthermore, the proximity of the core location to the Ganges-Brahmaputra and Mahanadi river mouths and documentation of very low percentages of $CaCO_3$ values indicate that $CaCO_3$ at this location could be primarily controlled by terrigenous dilution. Secondly, primary productivity at these river mouths is influenced by the fresh water discharges and sediment suspension during the SWM. The main source of terrigenous supply to the core site is the peninsular rivers such as Mahanadi and Krishna-Godavari and Ganges-Brahmaputra with most of the sediment supply occurring during the SW monsoon followed by NE monsoon season (Ittekkot et al. 1992). Therefore, the variations of $CaCO_3$ and MS at this core location represent the terrigenous dilution that is tightly coupled with the monsoon strength.

$CaCO_3$ and MS follow a very similar trend over the last ~80 kyr, they both exhibit high values in glacial periods MIS 4 & 2, and low values in interglacial periods MIS 5a & 1, except 3. Increased $CaCO_3$ content during glacials MIS 4 & 2 could be attributed to the higher primary productivity. Previous studies such as Phillips et al. (2014) have documented that during the last glacial when SWM was weakened, there was an elevated Aeolian Asian dust fluxes and increased the salinity of BoB, and the decreased freshwater input over this period likely diminished stratification allowing for increased mixing and nutrient availability thus enhancing productivity. Another possible factor for enhanced $CaCO_3$ content during this period may be attributed to the lower sea level (~120 m), which allowed erosion of the exposed carbonaceous continental shelf and draining of suspended river load directly into the deep sea (Pattan et al. 2003). This is supported by the increased MS, Ti and Al values (Fig. 3) inferring increased terrigenous input during the glacial episodes (MIS 4 & 2). Similarly more terrigenous organic matter supply to the BoB was reported during MIS 2 (Bhushan et al. 2007). The Magnetic Susceptibility values in the western BoB were reported to be controlled by the relative contribution of sediments from Ganges-Brahmaputra and the Peninsular river systems (Tripathy et al. 2011). These river systems drain sediments from different source regions of different rock compositions. Significantly higher MS values of fluvial sediments from Peninsular Indian regions were reported in the Bengal Fan (Sangode et al. 2001) because Peninsular Deccan basalts are rich in titanomagnetite with minor hematite (Courtillot et al. 1986) unlike those from the Himalayan basins (Sangode et al. 2001). Therefore, weakening of SWM during MIS 4 and 2 resulting in lesser SWM related run-off from the Ganges-Brahmaputra to the present study region must have attributed to the increased MS values owing to the relative enhancement of sediment supply from the Peninsular rivers.

During the interglacials on the other hand, for instance, low $CaCO_3$ and low MS during MIS 5a and 1 (Fig. 3) suggests more terrigenous dilution from the SWM-induced supply through Ganges-

Formatted: No underline, (Complex) Arabic (Saudi Arabia), English (United Kingdom)

Formatted: No underline, Font color: Custom Color(RGB(0,0,10)), (Complex) Arabic (Saudi Arabia), English (United Kingdom)

Formatted: No underline, Font color: Custom Color(RGB(0,0,10)), (Complex) Arabic (Saudi Arabia), English (United Kingdom)

Formatted: No underline, (Complex) Arabic (Saudi Arabia), English (United Kingdom)

Formatted: No underline, Font color: Custom Color(RGB(0,0,10)), (Complex) Arabic (Saudi Arabia), English (United Kingdom)

Formatted: No underline, (Complex) Arabic (Saudi Arabia), English (United Kingdom)

Formatted: No underline, Font color: Custom Color(RGB(0,0,10)), (Complex) Arabic (Saudi Arabia), English (United Kingdom)

Formatted: No underline, (Complex) Arabic (Saudi Arabia), English (United Kingdom)

Formatted: No underline, Font color: Custom Color(RGB(0,0,10)), (Complex) Arabic (Saudi Arabia), English (United Kingdom)

Formatted: No underline, (Complex) Arabic (Saudi Arabia), English (United Kingdom)

Formatted: No underline, Font color: Custom Color(RGB(0,0,10)), (Complex) Arabic (Saudi Arabia), English (United Kingdom)

Formatted: No underline, (Complex) Arabic (Saudi Arabia), English (United Kingdom)

Formatted: No underline, Font color: Custom Color(RGB(0,0,10)), (Complex) Arabic (Saudi Arabia), English (United Kingdom)

Formatted: No underline, (Complex) Arabic (Saudi Arabia), English (United Kingdom)

Formatted: No underline, Font color: Custom Color(RGB(0,0,10)), (Complex) Arabic (Saudi Arabia), English (United Kingdom)

Formatted: No underline, Font color: Custom Color(RGB(0,0,10)), (Complex) Hindi, English (India)

Formatted: No underline, (Complex) Hindi, English (India)

Brahmaputra rivers. However, high $CaCO_3$ coincided with low MS values in MIS 3, and the relatively higher $CaCO_3$ content during MIS 3 than in MIS 5a and 1 reveals either less terrigenous dilution through Ganges-Brahmaputra rivers due to weaker SWM during MIS 3 compared to 5a and 1 (Anderson and Prell 1993; Rostek et al. 1993; Schulz et al. 1998; Govil and Naidu 2011; Joussain et al. 2016), and/or higher primary productivity as is also evident from a nearby core NGHP-01-19B for the period of ~70 to 10 ka, wherein, a weakened SWM under glacial conditions, resulted in decreased precipitation and river discharge, together increases the salinity of the surface waters in Bay of Bengal, thereby increasing the biological primary productivity through weakened stratification over the BoB allowing for more mixing (Phillips et al. 2014). The transition of MIS 3 to MIS 2 show increased values of both $CaCO_3$ and MS with MIS 2 recording the highest average values of both $CaCO_3$ and MS. Highest peaks of MS at ~26.8 and ~19.7 kyr may be inferred to reflect periods of least dilution from SWM-induced river discharge from Ganges-Brahmaputra and highest primary productivity. A very likely source for the high values of MS during MIS 2 (LGM) is the relatively enhanced contribution of sediments from the Peninsular Indian regions (Tripathy et al. 2011) rather than Ganges-Brahmaputra while SWM is weakened (Joussain et al. 2016). A similar trend of high MS values during LGM in the western Bengal Fan was also reported by Sangode et al. (2001) and this change was attributed to the weakening of sediment contribution from the Himalayan rivers. Ti and Al values also show a reduced trend of terrigenous supply during LGM supporting the inference, and less dilution by non-carbonaceous terrigenous input might have resulted in the high $CaCO_3$ content along with the increased productivity during cold LGM. This suggests a weakening of SWM and/or intensification of NEM during this period. This is in agreement with various studies that have demonstrated that SWM was weaker (stronger) during the colder (warmer) periods with minimum intensity of SWM during the LGM (Schulz et al. 1998; Kudrass et al. 2001; Sinha et al. 2005; Gupta et al. 2011; Tiwari et al. 2011). Others have also inferred weaker SWM and stronger NEM during the LGM than the present day (Duplessy 1982; Prell 1984; Naidu and Malmgren 1995, 2005; Overpeck et al. 1996). The weak SWM (strong NEM) during LGM is also supported by enriched $\delta^{18}O$ values from the BoB (Govil and Naidu, 2011; Rashid et al. 2011) suggesting that the Indian summer monsoon was weakest during these periods and the climate was much drier, inducing less Ganges-Brahmaputra-Mahanadi (GBM) outflow and/or less overhead precipitation in BoB (Kudrass et al. 2001; Rashid et al. 2011).

Towards the end of MIS 2, monsoon has been reported to fluctuate widely with weaker monsoons during colder (NEM-dominated) episodes such as Younger Dryas (YD) and stronger monsoons during warmer (SWM-dominated) episodes such as Bølling-Allerød (B/A) (Sirocko et al.

Formatted: No underline, Font color: Custom Color(RGB(0,0,10))

Formatted: No underline, (Complex) Hindi, English (India)

Formatted: No underline, Font color: Custom Color(RGB(0,0,10)), (Complex) Hindi, English (India)

Formatted: No underline, (Complex) Hindi, English (India)

Formatted: No underline, Font color: Custom Color(RGB(0,0,10)), (Complex) Arabic (Saudi Arabia), English (United Kingdom)

Formatted: No underline, (Complex) Arabic (Saudi Arabia), English (United Kingdom)

1993; Kudrass et al. 2001; Rashid et al. 2011). Our records also reflect similar fluctuations through the later part of MIS 2 till mid-MIS 1. MS decreased from ~19.7 to ~16.3 kyr with a brief increase from ~16.3 kyr to ~14.3 kyr and continued with a steep decrease ~14.3 to ~11 kyr. These are synchronous with the steep decrease of $CaCO_3$ from ~16 to ~9 kyr probably due to increased dilution from Ganges-Brahmaputra discharge, marking the onset of SWM strengthening phase. This also coincided with the rapid warming during B/A which is consistent with the record from western BoB wherein an overall ~3.5°C rise in SST was documented from 17 to 10 kyr with the onset of SWM strengthening phase reported at ~14.7 kyr during B/A (Govil and Naidu 2011), and of rainfall maximum in northern India and river discharge into the BoB from 15.8 to 12.8 kyr as documented in the speleothem $\delta^{18}O$ from Timta cave (Sinha et al. 2005). However, our proxy records do not prominently mark these events rather just capture their increasing, decreasing and/or breaking trend, (probably) due to their resolution and/or insignificant preservation of the signals due to some other influencing processes at the core location.

Decreasing trend of MS and $CaCO_3$ content observed during the transition of MIS 2 to 1 continuing till mid-MIS 1 suggests an increase in SWM intensity during the period (Govil and Naidu, 2010). This must have enhanced the contribution of sediments from the Himalayan-derived Ganges-Brahmaputra while the contribution from the Peninsular rivers was subdued resulting in low MS values and $CaCO_3$ content. The most depleted $\delta^{18}O$ values are reported for the same period suggesting that it was the wettest period with the strongest Indian summer monsoon that resulted in a drastic precipitation increase in the catchments of the Ganga-Brahmaputra-Mahanadi river systems and/or more direct precipitation in the BoB (Rashid et al. 2011). This is consistent with other records in and around Arabian Sea (Fleitmann et al. 2003; Gupta et al. 2005) and Andaman Sea (Rashid et al. 2007) for the period. However, the MS and $CaCO_3$ data do not reflect these smaller events most probably because of its resolution, except for the decreasing trend as SWM intensified through the end of MIS 2 to mid-MIS 1 i.e. from ~16 to ~7 kyr. Although Ba profile shows high productivity, $CaCO_3$ values remained low for the whole MIS 1 possibly due to dominating influence of terrigenous dilution over the productivity. Goodbred and Kuehl (2000) found that when the SWM was strong around 11 to 7 kyr, ~5 x 10^{12} m^3 of sediment was reported to be deposited in the BoB. Thus, the high SWM-induced discharge obviously must have been responsible for dilution at the core location resulting in the low values of $CaCO_3$ during MIS 1. From mid- to late-MIS 1, the $CaCO_3$ values are invariably low but on the other hand, MS record shows a gradual, increasing trend during the period suggesting that SWM might have been weakening gradually since mid-Holocene with repeated occurrence of dry phases while NEM has been slowly getting intensified comparatively. This

Formatted: No underline, Font color: Custom Color(RGB(0,0,10)), (Complex) Arabic (Saudi Arabia), English (United Kingdom)

Formatted: No underline, (Complex) Arabic (Saudi Arabia), English (United Kingdom)

Formatted: No underline, Font color: Custom Color(RGB(0,0,10)), (Complex) Arabic (Saudi Arabia), English (United Kingdom)

Formatted: No underline, Font color: Custom Color(RGB(0,0,10)), (Complex) Arabic (Saudi Arabia), English (United Kingdom)

Formatted: No underline, (Complex) Arabic (Saudi Arabia), English (United Kingdom)

Formatted: No underline, Font color: Custom Color(RGB(0,0,10)), (Complex) Arabic (Saudi Arabia), English (United Kingdom)

Formatted: No underline, (Complex) Arabic (Saudi Arabia), English (United Kingdom)

Formatted: No underline, Font color: Custom Color(RGB(0,0,10)), (Complex) Arabic (Saudi Arabia), English (United Kingdom)

inference too finds support in findings of other monsoon studies (Neff et al. 2001; Fleitmann et al. 2003, 2007; Gupta et al. 2003, 2005, 2011; Rashid et al. 2007, 2011; Achyuthan et al. 2014; Böll et al. 2015) from adjacent regions.

The interplay between SWM and NEM control on the terrigenous material supply to the BoB

The climatic variations recorded in our reconstructed $CaCO_3$, MS, Ti, Al and Ba data reflecting variations in the strength of SWM and NEM are in tandem with other long-term records as well, which have suggested distinct glacial-interglacial variability in monsoon intensity throughout the Pleistocene (Clemens and Prell 1991). Various proxy records from the Arabian Sea and BoB reveal strengthening (weakening) of SWM accompanied by possible weakening (intensification) of NEM during interglacials (colder glacials) and vice versa during glacial times (e.g., Duplessy 1982; Dahl and Oppo 2006); This coupling relationship between SWM and NEM observed seemed to have been contemporaneous with other global climatic changes.

The $CaCO_3$ and MS values of MIS 4 and MIS 3 oscillated with intermediate levels between the LGM and Holocene values, which are in agreement with the $\delta^{18}O$ values variability between 80 and 30 kyr rfrom the northern BoB (Kudrass et al. 2001). Our terrigenous supply proxy records, showing that the LGM is marked with weaker SWM over BoB, is not only consistent with other monsoon proxies from different regions of Indian Ocean but also echo with the weak East Asian summer monsoon-associated lowest precipitation in China as inferred from the Hulu, Donggee and Sanbao speleothems records (Wang et al. 2001, 2005; Dong et al. 2010), and the strongest winter monsoon from the mean grain size variation records from northwestern Chinese Loess Plateau (Sun et al. 2011) (Fig. 3). This period also recorded a higher supply of African wind-blown mineral dust from NW African to the neighbouring eastern tropical Atlantic Ocean (deMenocal et al. 2000; Mulitza et al. 2008). These findings also support that the Indian and East Asian monsoon systems are dynamically linked to each other and have undergone synchronous hydrological and climatic changes, which may even be linked to other tropical climate systems such as the African monsoons.

The last deglaciation witnessed a steep increase in the strength of SWM from ~16 to ~10 kyr as evident from the low $CaCO_3$ values, which is synchronous with reports from western BoB (Govil and Naidu 2011), Timta cave (Sinha et al. 2005), Hulu (Wang et al. 2001), and Dongge (Yuan et al. 2004). The intensification of SWM and decreasing strength of NEM in the early Holocene as evident from our terrigenous supply records ($CaCO_3$, MS, Ti and Al) parallel the high temperatures in the extratropical Northern Hemisphere (NH) (30°N to 90°N) (Marcott et al. 2013). The minimum MS values during this period reflect the strongest SWM and/or weakest NEM, implying a much higher

Formatted: No underline, (Complex) Arabic (Saudi Arabia), English (United Kingdom)

Formatted: No underline

Formatted: No underline, Font color: Custom Color(RGB(0,0,10)), (Complex) Arabic (Saudi Arabia), English (United Kingdom)

Formatted: No underline, Font color: Custom Color(RGB(0,0,10)), (Complex) Arabic (Saudi Arabia), English (United Kingdom)

Formatted: No underline, Font color: Custom Color(RGB(0,0,10)), (Complex) Arabic (Saudi Arabia), English (United Kingdom)

Formatted: No underline, (Complex) Arabic (Saudi Arabia), English (United Kingdom)

Formatted: No underline, Font color: Custom Color(RGB(0,0,10)), (Complex) Hindi, English (India)

Formatted: No underline, (Complex) Hindi, English (India)

Formatted: No underline, (Complex) Arabic (Saudi Arabia), English (United Kingdom)

river discharges into the BoB especially from the Himalayan river systems. This period was marked by strongest Indian summer monsoon (Rashid et al. 2011), higher East Asian summer monsoon-associated precipitation over Asian landmass and African Humid Period, warmer climate in the Tibetan Plateau and less supply of African mineral dust (deMenocal et al. 2000; Thompson et al. 2002, 2006; Wang et al. 2005), which are consistent with our results. In addition, the trend of decreasing temperatures in the NH from ~5.5 to 0.1 kyr, synchronous with strengthening NEM intensity over the northern Arabian Sea and East Asia (Yancheva et al. 2007) is also in agreement with our records which show SWM weakening (NEM strengthening) around mid-Holocene to present. This linkage was also recognized in other studies that related variations in summer monsoon strength with the NH climate during the Holocene (e.g. Sirocko et al. 1996; Gupta et al. 2003; Hong et al. 2003; Wang et al. 2005). Albeit the linkage being recognized, the mechanisms associated are still debated, and more high-resolution studies would be useful in identifying the mechanisms. However, we hypothesize that such a teleconnections between the NH climate and other wider climate systems including the Indian monsoon system is possible only through atmospheric mediation by the mean shift of ITCZ associated with the boundary conditions during the glacial-interglacial changes.

Conclusions

Reconstruction of $CaCO_3$ content, MS, Ba, Al and Ti concentrations from a northern BoB sediment core for the last ~80 kyr reveals that $CaCO_3$ and MS variations at the core location are mainly controlled by terrigenous dilution associated with monsoon-induced river discharges and source of sediment supply. Less $CaCO_3$ content associated with lower MS values during interglacials (MIS 5a and 1 except 3) represents that dilution of terrigenous material supply through Ganges and Brahmaputra was higher during interglacials due to stronger SWM. Whereas glacials (MIS 4 & 2) exhibit higher $CaCO_3$ and MS values which are attributed to higher primary productivity and/or carbonaceous terrigenous inputs derived from exposed continental shelf areas during lower sea level and less river discharge from the Himalayan rivers (Ganges-Brahmaputra) relative to sediment contribution from the Peninsular Indian rivers due to weakened SWM and stronger NEM. We conclude that a tight coupling existed between terrigenous matter supply through the major rivers into the Bay of Bengal and the strengths of SWM and NEM. Fluctuations of $CaCO_3$ and MS through the last ~80 kyr in the northern BoB are in tune with other climate records such as the Chinese loess and paleosols sequences, which reveals a strong coupling exists between the SWM and NEM and terrigenous material supply in both marine and terrestrial regions in the Asian Continent.

Formatted: No underline, Font color: Custom Color(RGB(0,0,10)), (Complex) Arabic (Saudi Arabia), English (United Kingdom)

Formatted: No underline, Font color: Custom Color(RGB(0,0,10)), (Complex) Hindi, English (India)

Formatted: No underline, (Complex) Hindi, English (India)

Formatted: No underline, Font color: Custom Color(RGB(0,0,10)), (Complex) Hindi, English (India)

Acknowledgements

Authors thank all the participants of cruise MD 161 for providing the samples and Director, CSIR-National Institute of Oceanography, Goa, for his constant support and encouragement. Dr. Siby Kurian is gratefully acknowledged for her help with ICP-OES. C. Panmei acknowledges CSIR for providing Senior Research Fellowship. This work is funded by the Ministry of Earth Sciences (MoES) grant to P. D. Naidu. Data can be accessed through the supplementary material provided.

Compliance with ethical standards

Conflict of interest: The authors declare that there is no conflict of interest with third parties.

Formatted: Font: 12 pt, Complex Script Font: 12 pt

Formatted: No underline, Font color: Custom Color(RGB(0,0,10)), (Complex) Hindi, English (India)

Formatted: Font: 12 pt, Complex Script Font: 12 pt

Formatted: Space After: 6 pt

Formatted: No underline, Font color: Custom Color(RGB(0,0,10)), (Complex) Hindi, English (India)

Formatted: Justified, Space After: 6 pt

References

Achyuthan H, Nagasundaram M, Gourlan AT, Eastoe C, Ahmad SM, Padmakumari VM (2014) Mid-Holocene Indian Summer Monsoon variability off the Andaman Islands, Bay of Bengal. Quat Int 349:232–244. doi:10.1016/j.quaint.2014.07.041

Ahmad SM, Padmakumari VM, Babu GA (2009) Strontium and neodymium isotopic compositions in sediments from Godavari, Krishna and Pennar rivers. Curr. Sci. 97 (12):1766-1769

Anderson DM, Prell WL (1993) A 300 kyr record of upwelling off Oman during the Late Quaternary: Evidence of the Asian Southwest Monsoon. Paleoceanography 8:193–208. doi:10.1029/93PA00256

Anon (1993) Anthropogenic influences on sediment discharge to the coastal zone and environmental consequences. GESAMP Reports And Studies No. 52, 67 pp

Böll A, Schulz H, Munz PM, Rixen T, Gaye B, Emeis KC (2015) Contrasting sea surface temperature of summer and winter monsoon variability in the northern Arabian Sea over the last 25ka. Palaeogeogr Palaeoclimatol Palaeoecol 426:10–21. doi:10.1016/j.palaeo.2015.02.036

Carver RE (ed) (1971) Procedures in sedimentary petrology. Wiley-Intersci., New York, USA

Chao, W.C., 2000. Multiple Quasi Equilibria of the ITCZ and the origin of monsoon onset. J. Atmos. Sci. 57, 641e651.

Chao, W.C., Chen, B., 2001. The origin of monsoons. J. Atmos. Sci. 58, 3497e3507.

Chen J, Farrell JW, Murray DW, Prell WL (1995) Timescale and paleoceanographic implications of a 3.6 m.y. oxygen isotope record from the northeast Indian Ocean (Ocean Drilling Program Site 758). Paleoceanography10:21–47. doi:10.1029/94PA02290

Clemens SC, Prell WL (1991) One-million year record of summer-monsoon winds and continental aridity from the Owen Ridge (Site 722B), northwest Arabian Sea. Ocean Drill Prog Sci Res 117:365-388

Colin C, Kissel C, Blamart D, Turpin L (1998) Magnetic properties of sediments in the Bay of Bengal and the Andaman Sea: Impact of rapid North Atlantic Ocean climatic events on the strength of the Indian monsoon. Earth Planet Sci Lett 160, 623-635

Courtillot V, Besse J, Vandamme D, Montigny R, Jaeger J, Cappetta H (1986) Deccan flood basalts and the Cretaceous/Tertiary boundary. Earth Planet Sci Lett 80:361–374. doi:10.1038/333843a0

Dahl KA, Oppo DW (2006) Sea surface temperature pattern reconstructions in the Arabian Sea. Paleoceanography 21, PA1014, doi:10.1029/2005PA001162

Damuth JE (1975) Quaternary climate change as revealed by calcium carbonate fluctuations in western Equatorial Atlantic sediments. Deep Sea Res Oceanogr Abstr22:725–743. doi:10.1016/0011-7471(75)90078-9

deMenocal P (2000) Coherent high- and low-latitude climate variability during the Holocene warm period. Science 288:2198–2202. doi:10.1126/science.288.5474.2198

deMenocal P, Bloemendal J, King J (1991) A rock-magnetic record of monsoonal dust deposition to the Arabian Sea: Evidence for a shift in the mode of depostion at 2.4 Ma. Proc Ocean Drill Program Sci Results 117:389–407

Dong J, Wang Y, Cheng H, Hardt B, Edwards RL, Kong X, Wu J, Chen S, Liu D, Jiang X, Zhao K (2010) A high-resolution stalagmite record of the Holocene East Asian monsoon from Mt Shennongjia, central China. Holocene 20:257–264. doi:10.1177/0959683609350393

Formatted: No underline, Font color: Custom Color(RGB(0,0,10)), (Complex) Hindi, English (India)

Formatted: Space After: 6 pt, Line spacing: single

Formatted: No underline, Font color: Custom Color(RGB(0,0,10)), (Complex) Hindi, English (India)

Formatted: No underline, Font color: Custom Color(RGB(0,0,10)), (Complex) Hindi, English (India)

Formatted: No underline, Font color: Custom Color(RGB(0,0,10)), (Complex) Hindi, English (India)

Formatted: No underline, Font color: Custom Color(RGB(0,0,10)), (Complex) Hindi, English (India)

Formatted: No underline, Font color: Custom Color(RGB(0,0,10)), (Complex) Hindi, English (India)

Formatted: No underline, Font color: Custom Color(RGB(0,0,10))

Formatted: Justified, Space After: 6 pt, Line spacing: single

Formatted: No underline, Font color: Custom Color(RGB(0,0,10))

Formatted: Space After: 6 pt, Line spacing: single

Formatted: No underline, Font color: Custom Color(RGB(0,0,10)), (Complex) Hindi, English (India)

Duplessy JC (1982) Glacial to interglacial contrast in the northern Indian Ocean. Nature 295:494–498. doi:10.1038/295494a0

Fleitmann D, Burns SJ, Mudelsee M, Neff U, Kramers J, Mangini A, Matter A (2003) Holocene forcing of the Indian monsoon recorded in a stalagmite from southern Oman. Science 300:1737–1739. doi:10.1126/science.1083130

Gomes HR, Goes JI, Saino T (2000) Influence of physical processes and freshwater discharge on the seasonality of phytoplankton regime in the Bay of Bengal. Cont. Shelf Res. 20: 313-330

Goodbred SL, Kuehl SA (2000) The significance of large sediment supply, active tectonism, and eustasy on margin sequence development: Late Quaternary stratigraphy and evolution of the Ganges-Brahmaputra delta. Sediment Geol 133:227–248. doi:10.1016/S0037-0738(00)00041-5

Govil P, Naidu PD (2011) Variations of Indian monsoon precipitation during the last 32kyr reflected in the surface hydrography of the Western Bay of Bengal. Quat Sci Rev 30:3871–3879. doi:10.1016/j.quascirev.2011.10.004

Govil P, Naidu PD (2010) Evaporation-precipitation changes in the eastern Arabian Sea for the last 68 ka: Implications on monsoon variability. Paleoceanography 25:1–19. doi:10.1029/2008PA001687

Gupta AK, Das M, Anderson DM (2005) Solar influence on the Indian summer monsoon during the Holocene. Geophys Res Lett 32, L17703. doi:10.1029/2005GL022685

Gupta AK, Anderson DM, Overpeck JT (2003) Abrupt changes in the Asian southwest monsoon during the Holocene and their links to the North Atlantic Ocean. Nature 421:354–357. doi:10.1038/nature01340

Gupta AK, Mohan K, Sarkar S, Clemens SC, Ravindra R, Uttam RK (2011) East–West similarities and differences in the surface and deep northern Arabian Sea records during the past 21Kyr. Palaeogeogr Palaeoclimatol Palaeoecol 301:75–85. doi:10.1016/j.palaeo.2010.12.027

Hastenrath S, Lamb P.J (1979) Climatic Atlas of the Indian Ocean, Part 1: Surface Climate and Atmospheric Circulation. University of Wisconsin Press, Madison, Wisconsin

Hong YT, Hong B, Lin QH, Zhu YX, Shibata Y, Hirota M, Uchida M, Leng XT, Jiang HB, Xu H, Wang H, Yi L (2003) Correlation between Indian Ocean summer monsoon and North Atlantic climate during the Holocene. Earth Planet Sci Lett 211:371–380. doi:10.1016/S0012-821X(03)00207-3

Ittekkot V, Haake B, Bartsch M, Nair RR, Ramaswamy V (1992) Organic carbon removal in the sea: the continental connection. Geological Society, London, Special Publications 64167-176. doi:10.1144/GSL.SP.1992.064.01.11

Joussain R, Colin C, ….. Bassinot F (2016) Climatic control of sediment transport from the Himalayas to the proximal NE Bengal during th last glacial-interglacial cycle. Quat. Sci. Rev. 148, 1-16

Kent DV (1982) Apparent correlation of palaeomagnetic intensity and climatic records in deep-sea sediments. Nature 296:538–539. doi:10.1038/299538a0

Kolla V, Be AWH, Bisca ye PE (1976) Calcium carbonate distribution in the surface sediments of the Indian Ocean. J Geophys Res 81:2605-2616. doi:10.1029/JC081i015p02605

Kudrass HR, Hofmann A, Doose H, Emeis K, Erlenkeuser H (2001) Modulation and amplification of climatic changes in the Northern Hemisphere by the Indian summer monsoon during the past 80 k.y. Geology 29:63–66. doi:10.1130/0091-7613(2001)029<0063:MAAOCC>2.0.CO;2

Formatted: Font: Times New Roman, 12 pt, No underline, Font color: Custom Color(RGB(0,0,10)), Complex Script Font: 12 pt, (Complex) Hindi, English (India)

Formatted: No underline, (Complex) Hindi, English (India)

Formatted: No underline, (Complex) Hindi, English (India)

Formatted: No underline, (Complex) Hindi, English (India)

Formatted: Font: Times New Roman, 12 pt, No underline, Font color: Custom Color(RGB(0,0,10)), Complex Script Font: 12 pt, (Complex) Hindi, English (India)

Formatted: No underline, (Complex) Hindi, English (India)

Kumar Anil A, Rao VP, Patil SK, Kessarkar PM, Thamban,M (2005) Rock magnetic records of the sediments of the eastern Arabian Sea: Evidence for late Quaternary climatic change. Mar Geol 220:59–82. doi:10.1016/j.margeo.2005.06.038

Madhupratap M, Gauns M, Ramaiah N, Kumar SP, Muraleedharan PM, de Souza SN, Sardessai S, Muraleedharan U (2003) Biogeochemistry of the Bay of Bengal: physical, chemical and primary productivity characteristics of the central and western Bay of Bengal during the summer monsoon 2001. Deep Sea Res. Part II 50:881-896

Marcott SA, Shakun JD, Clark PU, Mix AC (2013) A reconstruction of regional and global temperature for the past 11,300 years. Science 339:1198–201. doi:10.1126/science.1228026

Milliman JD, Meade RH (1983) World-Wide Delivery of River Sediment to the Oceans. J Geol 91:1–21. doi:10.1086/628741

Mulitza S, Prange M, Stuut JB, Zabel M, Von Dobeneck T, Itambi AC, Nizou J, Schulz M, Wefer G (2008). Sahel megadroughts triggered by glacial slowdowns of Atlantic meridional overturning. Paleoceanography 23:1–11. doi:10.1029/2008PA001637

Naidu PD (1991) Glacial to interglacial contrasts in the calcium carbonate content and influence of Indus discharge in two eastern Arabian Sea cores. Palaeogeogr Palaeoclimatol Palaeoecol 86:255-264. doi:10.1016/0031-0182(91)90084-5

Naidu PD, Malmgren BA (1995) A 2,200 years periodicity in the Asian monsoon system. Geophys Res Lett 22:2361–2364. doi:10.1029/95gl02558

Neff U, Burns SJ, Mangini A, Mudelsee M, Fleitmann D, Matter A (2001) Strong coherence between solar variability and the monsoon in Oman between 9 and 6 kyr ago. Nature 411:290–293. doi:10.1038/35077048

Overpeck J, Anderson D, Trumbore S, Prell W (1996) The southwest Indian Monsoon over the last 18000 years. Clim Dyn 12:213–225. doi:10.1007/BF00211619

Pattan JN, Masuzawa T, Naidu PD, Parthiban G, Yamamoto M (2003) Productivity fluctuations in the southeastern Arabian Sea during the last 140 ka. Palaeogeogr Palaeoclimatol Palaeoecol 193:575–590. doi:10.1016/S0031-0182(03)00267-0

Phillips SC, Johnson JE, Giosan L, Rose K (2014) Monsoon-induced variation in productivity and lithogenic sediment flux since 110 ka in the offshore Mahanadi Basin, northern Bay of Bengal. Mar and Petr. Geo. 58, 502-525

Prasanna Kumar S, Muraleedharan PM, Prasad TG, Gauns M, Ramaiah N, de Souza SN, Sardessai S, Madhupratap M (2002) Whys is the Bay of Bengal less productive during summer monsoon compared to the Arabian Sea? Geophys. Res. Lett. 29. http://dx.doi.org/10.1029/2002GL016013

Prell WL (1984) Variation of Monsoonal Upwelling: A Response to Changing Solar Radiation. In: Climate Processes and Climate Sensitivity. pp. 48–57. doi:10.1029/GM029p0048

Rao K L (1979) India' s water wealth: Its assessment, uses and projections. Orient Longman Ltd, New Delhi.

Rao VP, Kessarkar PM, Patil SK, Ahmad S.M (2008) Rock magnetic and geochemical record in a sediment core from the eastern Arabian Sea: Diagenetic and environmental implications during the late Quaternary. Palaeogeogr Palaeoclimatol Palaeoecol 270:46–52. doi:10.1016/j.palaeo.2008.08.011

Formatted: Font: Times New Roman, 12 pt, No underline, Font color: Custom Color(RGB(0,0,10)), Complex Script Font: 12 pt, (Complex) Hindi, English (India)

Formatted: No underline, Font color: Custom Color(RGB(0,0,10)), (Complex) Hindi, English (India)

Formatted: No underline, Font color: Custom Color(RGB(0,0,10)), (Complex) Hindi, English (India)

Formatted: No underline, Font color: Custom Color(RGB(0,0,10)), (Complex) Hindi, English (India)

Formatted: No underline, Font color: Custom Color(RGB(0,0,10)), (Complex) Hindi, English (India)

Rao VP, Kessarkar PM, Thamban M. Patil SK (2010) Paleoclimatic and diagenetic history of the late quaternary sediments in a core from the Southeastern Arabian Sea: Geochemical and magnetic signals. J Oceanogr 66:133–146. doi:10.1007/s10872-010-0011-2

Rashid H, England E, Thompson L, Polyak L (2011) Late Glacial to Holocene Indian summer monsoon variability based upon sediment records taken from the Bay of Bengal. Terr Atmos Ocean Sci 22:215–228. doi:10.3319/TAO.2010.09.17.02(TibXS)

Rashid H, Flower BP, Poore RZ, Quinn T.M (2007) A ~25 ka Indian Ocean monsoon variability record from the Andaman Sea. Quat Sci Rev 26:2586–2597. doi:10.1016/j.quascirev.2007.07.002

Reimer P J, Baillie MGL, Bard E et al (2009) IntCal09 and Marine09 radiocarbon age calibration curves, 0–50,000 years cal BP. Radiocarbon 51(4):1111–1150. https://doi.org/10.1017/S0033822200034202

Rostek F, Ruhland G, Bassinot FC, Muller PJ, Labeyrie LD, Lancelot Y, Bard E (1993). Reconstructing sea-surface temperature and salinity using δ^{18}O18 and alkenone records. Nature 364:319–321. doi:Doi 10.1038/364319a0

Sager W, Hall S (1990) Magnetic properties of black mud turbidites from ODP Leg 116, Distal Bengal Fan, Indian Ocean. Proc Ocean Drill Program Sci Results 116:317–336

Sangode S, Suresh N, Bagati TN (2001). Godavari source in the Bengal fan sediments: Results from magnetic susceptibility dispersal pattern. Curr Sci 80:660–664

Sangode SJ, Sinha R, Phartiyal B, Chauhan OS, Mazari RK, Bagati TN, Suresh N, Mishra S, Kumar R, Bhattacharjee P (2007) Environmental magnetic studies on some Quaternary sediments of varied depositional settings in the Indian sub-continent. Quat Int 159:102–118. doi:10.1016/j.quaint.2006.08.015

Schlitzer R (2016) Ocean Data View. http://odv.awi.de

Schott FA, McCreary Jr. JP (2001) The monsoon circulation of the Indian Ocean. Progress in Oceanography, 51, 1-123

Schulz H, van Rad U, Erlenkeuser H (1998) Correlation between Arabian Sea and Greenland climate oscillations of the past 110,000 years. Nature 393:54–57. doi:10.1038/31750

Sengupta D, Bharath Raj GN, Shenoi SSC (2006) Surface freshwater from Bay of Bengal runoff and Indonesian Throughflow in the tropical Indian Ocean. Geophys. Res. Lett., 33(22), 1–5, doi:10.1029/2006GL027573

Shetye SR, Gouveia AD, Shenoi SSC, Sundar D, Michael GS, Nampoothiri G (1993) The western boundary current of the seasonal subtropical gyre in the Bay of Bengal. J Geophys Res 98:945-954. doi:10.1029/92JC02070

Sinha A, Cannariato KG, Stott LD, Li HC, You CF, Cheng H, Edwards RL, Singh IB (2005) Variability of southwest Indian summer monsoon precipitation during the Bølling-Ållerød. Geology 33:813–816. doi:10.1130/G21498.1

Sirocko F, Garbe-Schonberg D, McIntyre A, Molfino B (1996) Teleconnections between the subtropical monsoons and high-latitude climates during the last deglaciation. Science 272:526–529. doi:10.1126/science.272.5261.526

Sirocko F, Sarnthein M, Erlenkeuser H, Lange H, Arnold M, Duplessy JC (1993) Century-scale events in monsoonal climate over the past 24,000 years. Nature 364:322–324. doi:10.1038/364322a0

Formatted: No underline, Font color: Custom Color(RGB(0,0,10)), (Complex) Hindi, English (India)

Formatted: No underline, Font color: Custom Color(RGB(0,0,10)), (Complex) Hindi, English (India)

Formatted: No underline, Font color: Custom Color(RGB(0,0,10)), (Complex) Hindi, English (India)

Formatted: No underline, Font color: Custom Color(RGB(0,0,10)), (Complex) Hindi, English (India)

Formatted: No underline, Font color: Custom Color(RGB(0,0,10)), (Complex) Hindi, English (India)

Southon J, Kashgarian M, Fontugne M, Metivier B, Yim WWS (2002) Marine reservoir corrections for the Indian Ocean and Southeast Asia. Radiocarbon 44:167–180. doi:10.1017/S0033822200064778

Stuiver M, Reimer PJ (1993) Extended ^{14}C data base and revised CALIB 3.0 ^{14}C age calibration program. Radiocarbon 35:215–230. doi:10.1017/S0033822200013904

Subramanian V (1985) Geochemistry of river basins in the Indian Subcontinent, Part I: Water chemistry, chemical erosion and water-mineral equilibria. In: Transport of carbon and minerals in major world rivers. Part 3, ed ET Degens and S Kempe 58:495-512, Mittilungen aus dem Geologisch-Palaeontologischen, Institut der Universitat Hamburg

Sun Y, Clemens SC, Morrill C, Lin X, Wang X, An Z (2011) Influence of Atlantic meridional overturning circulation on the East Asian winter monsoon. Nat Geosci 5:46–49. doi:10.1038/ngeo1326

Thompson LG, Mosley-Thompson E, Brecher H, Davis M, León B, Les D, Lin PN, Mashiotta T, Mountain K (2006) Abrupt tropical climate change: Past and present. Proc Natl Acad Sci 103:10536–10543. doi:10.1073/pnas.0603900103

Thompson LG, Mosley-Thompson E, Davis ME, Henderson KA, Brecher HH, Zagorodnov VS, Mashiotta TA, Lin PN, Mikhalenko VN, Hardy DR, Beer J (2002) Kilimanjaro ice core records: evidence of Holocene climate change in tropical Africa. Science 298:589–593. doi:10.1126/science.1073198

Tiwari M, Singh AK, Ramesh R (2011) High-resolution monsoon records since Last Glacial Maximum: A comparison of marine and terrestrial paleoarchives from South Asia. J Geol Res 2011:1–12. doi:10.1155/2011/765248

Totland M, Jarvis I, Jarvis KE (1992) An assessment of dissolution techniques for the analysis of geological samples by plasma spectrometry. Chemical Geology 95:35-62. doi:10.1016/0009-2541(92)90042-4

Tripathy GR, Singh SK, Bhushan R, Ramaswamy V (2011) Sr–Nd isotope composition of the Bay of Bengal sediments. Geochem J 45:175–186. doi:10.2343/geochemj.1.0112

UNESCO (1971) Discharge of selected rivers of the world. UNESCO, Paris

Wang Y, Cheng H, Edwards RL, He Y, Kong X, An Z, Wu J, Kelly MJ, Dykoski CA, Li X (2005) The Holocene Asian monsoon: links to solar changes and North Atlantic climate. Science 308:854–857. doi:10.1126/science.1106296

Wang YJ, Cheng H, Edwards RL, An ZS, Wu JY, Shen CC, Dorale J A (2001) A high-resolution absolute-dated late Pleistocene Monsoon record from Hulu Cave, China. Science 294:2345–2348. doi:10.1126/science.1064618

Weber ME, Wiedicke-Hombach M, Kudrass HR, Erlenkeuser H (2003) Bengal Fan sediment fan transport activity and response to climate forcing inferred from sediment physical properties. Sed. Geo. 155, 361-381

Webster PJ, Magaña VO, Palmer TN, Shukla J, Tomas RA, Yanai M, Yasunari T (1998) Monsoons: Processes, predictability, and the prospects for prediction. J Geophys Res 103, 14451. doi:10.1029/97JC02719

Yancheva G, Nowaczyk NR, Mingram J, Dulski P, Schettler G, Negendank JFW, Liu J, Sigman DM, Peterson LC, Haug GH (2007) Influence of the intertropical convergence zone on the East Asian monsoon. Nature 445:74–7. doi:10.1038/nature05431

Formatted: No underline, Font color: Custom Color(RGB(0,0,10)), (Complex) Hindi, English (India)

Yuan D, Cheng H, Edwards RL, Dykoski CA, Kelly MJ, Zhang M, Qing J, Lin Y, Wang Y, Wu J, Dorale JA, An Z, Cai Y (2004) Timing, duration, and transitions of the last interglacial Asian monsoon. Science 304:575–578. doi:10.1126/science.1091220

List of figures

Formatted: Font: Times New Roman, 12 pt, No underline, Font color: Custom Color(RGB(0,0,10)), Complex Script Font: 12 pt, (Complex) Hindi, English (India)

Formatted: Normal

Formatted: Space After: 6 pt, Line spacing: single

Formatted: Normal, Centered

Formatted: Centered, Indent: Left: 0", Hanging: 0.33", Space After: 6 pt, Line spacing: single

Formatted: Font: 12 pt, Complex Script Font: 12 pt

Formatted: Font: Times New Roman, 12 pt, Complex Script Font: 12 pt

Formatted: Normal, Centered, No page break before

Formatted: Space After: 6 pt, Line spacing: single

Formatted: No underline, (Complex) Arabic (Saudi Arabia), English (United Kingdom)

Formatted: No underline, Font color: Custom Color(RGB(0,0,10)), (Complex) Hindi, English (India)

Formatted: No underline, (Complex) Hindi, English (India)

Formatted: No underline, (Complex) Hindi

Formatted: No underline, (Complex) Hindi, English (India)

Formatted: No underline, (Complex) Hindi

Formatted: No underline, (Complex) Hindi, English (India)

Formatted: No underline, (Complex) Hindi

Formatted: No underline, (Complex) Hindi, English (India)

Formatted: Justified, Space After: 6 pt, Line spacing: single

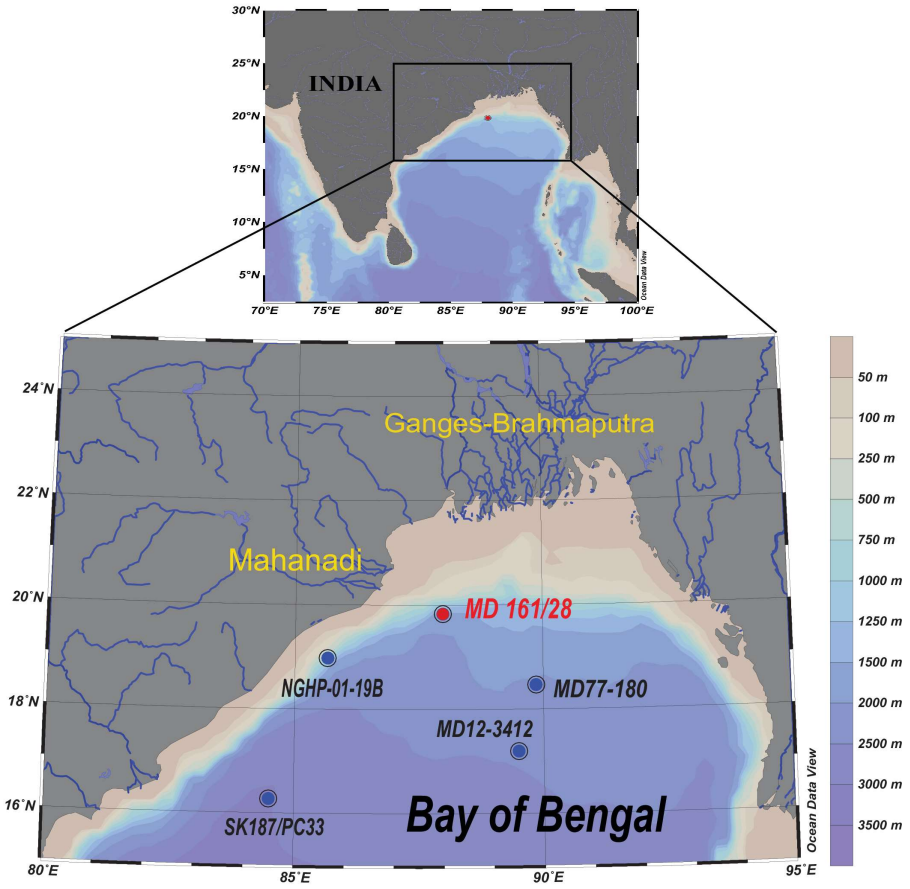

Fig. 1. Location of the core MD 161/28 used in this study and other cores discussed in text from the northern Bay of Bengal. Also shown are the Ganges-Brahmaputra and Mahanadi river drainage systems. The map was generated using Ocean Data View (Schlitzer, 2016).

Formatted: No underline, (Complex) Arabic (Saudi Arabia), English (United Kingdom)

Formatted: Line spacing: single

Formatted: Font: Not Bold, No underline, (Complex) Arabic (Saudi Arabia), English (United Kingdom)

Formatted: Font: Not Bold

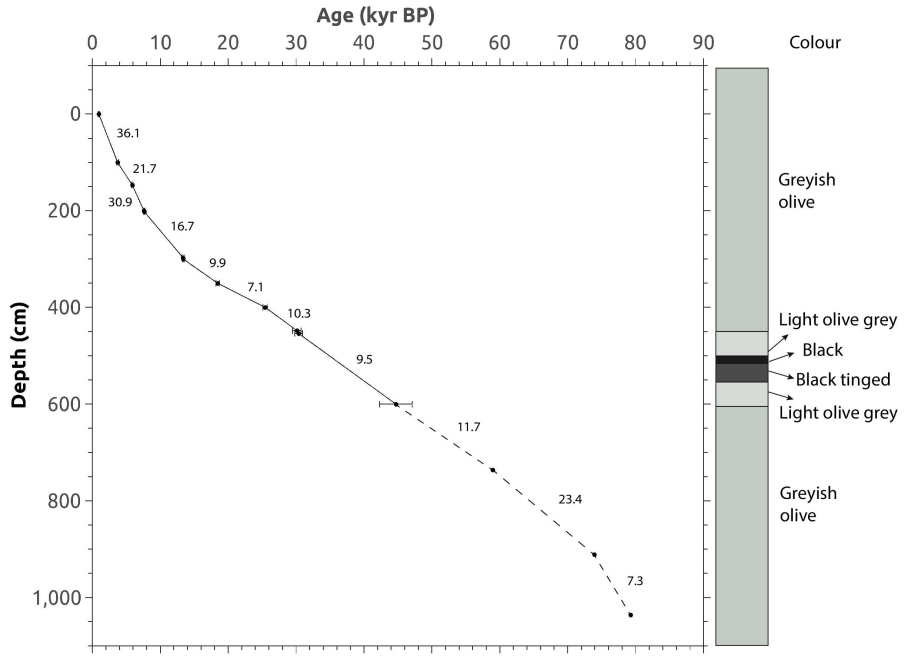

Fig. 2. Depth (cm) versus age (kyr BP) in the core MD 161/28 based on 12 AMS ^{14}C dates (solid dots with solid connecting lines), and 3 isotope stage-based ages (solid dots with dashed connecting lines). The ages are calibrated to calendar years using CALIB 7.1 program and Marine13 calibration curve (Stuiver and Reimer 1993; Reimer et al. 2013) with a correction for global reservoir effect of 400 years (Southon et al. 2002), and associated 2σ uncertainties are shown. Also shown is the downcore variation in sediment colour. Sedimentary rates in between the tie points are in cm/kyr.

Formatted: No underline

Formatted: No underline, (Complex) Hindi, English (India)

Formatted: Font: Not Bold, No underline, (Complex) Hindi, English (India)

Formatted: Space After: 6 pt, Line spacing: single

Formatted: Font: Not Bold

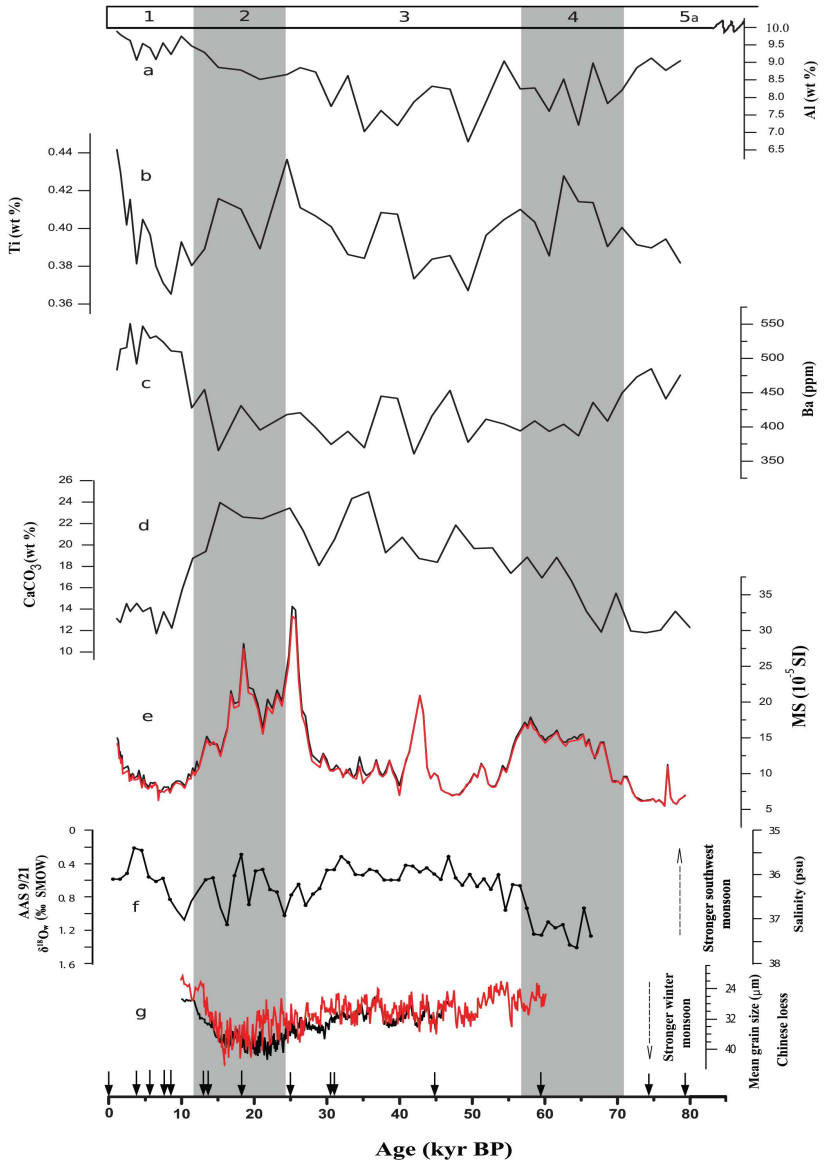

Fig. 3. Variations in (a) Al (wt %), (b) Ti (wt %), (c) Ba (ppm) (d) $CaCO_3$ (wt%) content, (e) magnetic susceptibility (MS) (10^{-5} SI) (black – low frequency; red – high frequency), and from the core MD 161/28 (present study), (f) $\delta^{18}O_w$ (‰) records from AAS 9/21 (Govil and Naidu, 2010), and (g) loess mean grain size (μm) from Gulang (red) and Jingyuan (black) (Sun et al., 2011). 1, 2, 3, 4

Formatted: Font: 12 pt, Complex Script Font: 12 pt

Formatted: No underline, (Complex) Hindi

Formatted: Space After: 6 pt, Line spacing: single

Formatted: No underline, (Complex) Hindi, English (India)

Formatted: No underline, (Complex) Hindi

Formatted: No underline, (Complex) Hindi, English (India)

Formatted: No underline, (Complex) Hindi

Formatted: No underline, (Complex) Hindi, English (India)

and 5a are Marine Isotope Stages (MIS). Arrows pointed to X axis are the age-control points (Table S1).

Page 6: [1] Formatted **User** **14-Feb-20 10:15:00 AM**

No underline, Font color: Custom Color(RGB(0,0,10)), (Complex) Arabic (Saudi Arabia), English (United Kingdom)

Page 6: [2] Formatted **User** **14-Feb-20 10:15:00 AM**

No underline, (Complex) Arabic (Saudi Arabia), English (United Kingdom)

Page 6: [3] Formatted **User** **14-Feb-20 10:15:00 AM**

No underline, Font color: Custom Color(RGB(0,0,10)), (Complex) Arabic (Saudi Arabia), English (United Kingdom)

Page 6: [4] Formatted **User** **14-Feb-20 10:15:00 AM**

No underline, (Complex) Arabic (Saudi Arabia), English (United Kingdom)

Page 6: [5] Formatted **User** **14-Feb-20 10:15:00 AM**

No underline, Font color: Custom Color(RGB(0,0,10)), (Complex) Arabic (Saudi Arabia), English (United Kingdom)

Page 6: [6] Formatted **User** **14-Feb-20 10:15:00 AM**

No underline, (Complex) Arabic (Saudi Arabia), English (United Kingdom)

Page 6: [7] Formatted **User** **14-Feb-20 10:15:00 AM**

No underline, Font color: Custom Color(RGB(0,0,10)), (Complex) Arabic (Saudi Arabia), English (United Kingdom)

Page 6: [8] Formatted **User** **14-Feb-20 10:15:00 AM**

No underline, Font color: Custom Color(RGB(0,0,10)), (Complex) Arabic (Saudi Arabia), English (United Kingdom)

Page 6: [9] Formatted **User** **14-Feb-20 10:15:00 AM**

No underline, Font color: Custom Color(RGB(0,0,10)), (Complex) Arabic (Saudi Arabia), English (United Kingdom)

Page 6: [10] Formatted **User** **14-Feb-20 10:15:00 AM**

No underline, (Complex) Arabic (Saudi Arabia), English (United Kingdom)

Page 6: [11] Formatted **User** **14-Feb-20 10:15:00 AM**

No underline, Font color: Custom Color(RGB(0,0,10)), (Complex) Arabic (Saudi Arabia), English (United Kingdom)

Page 6: [12] Formatted **User** **14-Feb-20 10:15:00 AM**

No underline, Font color: Custom Color(RGB(0,0,10)), (Complex) Arabic (Saudi Arabia), English (United Kingdom)

Page 6: [13] Formatted **User** **14-Feb-20 10:15:00 AM**

No underline, Font color: Custom Color(RGB(0,0,10)), (Complex) Arabic (Saudi Arabia), English (United Kingdom)

Page 6: [14] Formatted **User** **14-Feb-20 10:15:00 AM**

No underline, Font color: Custom Color(RGB(0,0,10)), (Complex) Arabic (Saudi Arabia), English (United Kingdom)

Page 6: [15] Formatted **User** **14-Feb-20 10:15:00 AM**

No underline, (Complex) Arabic (Saudi Arabia), English (United Kingdom)

Page 6: [16] Formatted **User** **14-Feb-20 10:15:00 AM**

No underline, Font color: Custom Color(RGB(0,0,10)), (Complex) Arabic (Saudi Arabia), English (United Kingdom)